# A Review Of The Effects And Mitigation Of Frost With Focus On Air-Source Heat Pump Applications

Amirarsalan Mashhadian

Tauseef Ismail

Christian K. Bach

Aaron Alexander

# A Review of the Effects and Mitigation of Frost with Focus on Air-source Heat Pump Applications

Amirarsalan MASHHADIAN[1], Tauseef ISMAIL[1], Christian K. BACH[1*], Aaron ALEXANDER[1]

[1]Oklahoma State University, Department of Mechanical and Aerospace Engineering,
Stillwater, Oklahoma, United States
Amashha@okstate.edu, Tismail@okstate.edu, Cbach@okstate.edu, Aaral@okstate.edu

* Corresponding Author

## ABSTRACT

Air source heat pumps (ASHPs) are commonly used to provide thermal comfort for both residential and commercial purposes and are seen as a key technology for the decarbonization of the built environment. However, frost forms on the outdoor coil (evaporator) under low temperature conditions. Frost reduces the heat transfer rate and efficiency of the ASHP, requiring energy costly defrosting processes. The frequency and impact of these defrosting processes can be reduced through frost retardation as well as the optimization of the defrost process and its initiation.

This review presents methods for retarding the onset of frosting, including changing the ambient conditions, modifying the system, adjusting the outdoor coil design, and exploiting external sources. As frost grows on the heat exchanger surface, heat exchanger capacity degrades, eventually requiring frost removal. Direct and indirect methods for evaluating frost severity were identified and classified into direct and indirect methods. Various defrosting techniques can be employed with reverse cycle defrosting (RCD) being most popular for commercial and residential ASHPs, followed by hot gas bypass defrosting (HGBD).

Defrosting is vital to maintaining ASHPs performance with robustness and simplicity of the controls being most critical for practical applications. Time-based defrosting control strategies are simple approach but cannot adapt well to changing ambient conditions. Advanced methods targeting optimal defrost initiation and process control are presented. Finally, we recommend areas for future research to increase ASHPs efficiency and climatic application range.

## 1. INTRODUCTION

Air source heat pumps (ASHPs) are energy-efficient devices that are widely used to provide thermal comfort for indoor spaces. In contrast to single-purpose air conditioning devices, ASHPs can provide both cooling and heating (Reiners et al., 2021). Reversible ASHPs transfer heat from outside to inside or inside to outside. While ASHPs are energy efficient heating devices, they may encounter frost build-up on their evaporator surface, reducing efficiency (Tang et al., 2020).

ASHP frosting starts to form on the outdoor coil when relative humidity is higher than 60% and ambient temperature is less than 5.5 °C (Jianhui et al., 2020). Surface temperature plays a critical role in frost build-up. Generally, at surface temperature is lower than both the ambient dew point and the freezing point, frost begins to form in stages: (1) Droplet condensation occurs, (2) Condensate droplets nucleate frost, (3) Frost crystals start to appear, and (4) Accumulation of multiple frost layers with different densities (Abbas & Woo, 2021).

Rafati et al. (2016) indicate that heat transfer rate slightly increased when condensation occurred but, once frost started to accumulate on the surface, the heat transfer decreased. The gaps between fins were also obstructed by frost which increased airside pressure drop and enlarged the thermal resistance between the airside and refrigerant side. Consequently, the thermal performance of the heat pump was reduced, increases the total energy consumption. Retarding methods and defrosting techniques are utilized to maintaining efficiency, a subset of which are covered subsequently.

Of the methods for frost retardation, system modifications, including surface coating and fin geometry alteration are the most prevalent in recently published literature(Mengjie et al., 2018). Although these methods cause a delay in frost build-up on the surface, defrosting is still required. In order to deploy defrosting techniques, frost existence must first be detected. Many frost detection methods have been proposed by researchers, and can be classified into three major types: (1) Direct, (2) Indirect, and (3) Model prediction based methods (Malik et al., 2020).

Defrosting is essential for maintaining equipment efficiency (Song et al., 2018). Reverse cycle defrosting (RCD) is the most common method used in current equipment followed by hot gas bypass defrosting (HGBD). However, the defrosting process cannot reduce energy consumption effectively unless the optimum time for defrosting initiation is found (Wang et al., 2013). Optimum defrost start time avoids mal-defrosting (undesirable time for starting defrosting) as well as excessive defrosting. Sometimes defrosting starts in an unsuitable condition, such as when no frost exists on the evaporator surface or the critical point for defrosting initiation is passed (Wang et al., 2011). Time-based methods are used extensively in heat pumps for defrosting initiation leading to mal-defrosting and wast energy compared to more complex approaches, such as using optical methods and artificial intelligence (Kim & Lee, 2015).

ASHPs, while energy efficient, often do not live up to their full potential due to frosting issues. Therefore, this paper presents the relevant frosting and defrosting topics. First, some retardation methods will be discussed because they can positively affect heat pumps performance by delaying defrosting. Frost detection methods will be presented as they are typically used for initiating the defrosting process. Defrosting methods and their controlling strategies will be elaborated upon as they are vital for heat pumps. Frosting and defrosting models are part of heat pumps' design stage optimization and way to be used for controls, so that this paper goes to explain these models.

## 2. FROST AND DEFROSTING MODELS

### 2.1 Frost Models

Frosting occurs on a surface when surface temperature is below the dew point of moist air and below 0°C. In many engineering applications, frosting is an undesired phenomenon as it reduces performance due to the low thermal conductivity of frost. The frost formation results in thermal and flow resistance, which adversely affect the performance of an ASHP. In the worst-case scenarios, frost can also lead to equipment failure. Thus, predicting frost growth and densification through models is a contemporary issue for engineering design.

A mathematical model was developed by Tao (1992) that predicted frost growth on a flat plate for ambient air conditions. Empirical correlations were derived to evaluate time variation of frost thickness, average frost density and heat flux using a finite difference method. Şahin (1995) performed an analytical study of frost formation as well as nucleation during the crystal growth period of frost formation. Basic principles of nucleation and crystallization were applied for modeling while the effect of surface temperature, inlet air temperature, humidity ratio and Reynolds number were examined. Lee et al. (1997) developed an analytical model by considering the molecular diffusivity of water vapor and the effect of heat transfer on the frost layer due to sublimation. The model was developed for frosting condition on a cold flat surface, while expressing the heat generation due to sublimation in terms of vapor density and absorption coefficient. The model predicted within 10% error for frost thickness when compared with experimental data and showed that frost surface temperature increased with increases in velocity and relative humidity of the air at the inlet.

Yun et al. (2002) presented a physics-based model for the growth and properties of frost layer over a flat plate at a subfreezing temperature. Empirical correlations were developed for frost roughness, heat and mass transfer coefficients, frost thermal conductivity, and the concentration of mass and densification of frost with time and space. It was observed that the flow pattern of air on the surface of frost was turbulent. Yang et al. (2006) presented a mathematical model for frosting on a cold plate. They found that turbulent flow boosts the frost formation in comparison to laminar flow. While on the other hand, the frost thickness increased with increase in air velocity under laminar flow. Kim et al. (2008) proposed dimensionless correlations for frost surface temperature, density, thickness, and heat transfer coefficient. The correlations were developed in terms of Reynolds number with a range of 700-3,000, and showed agreement with the experimental data within an error of 15%.

Negrelli & Hermes, (2015) developed an empirical model for thermal conductivity of frost on a flat surface. The model was based on experimental data from open literature for wall surface temperatures from -30ºC to -4ºC. The correlation for thermal conductivity was calculated in terms of porosity of the frosted medium. Brèque & Nemer

(2016) studied frost growth modeling based on diffusion through a porous media. The commonly used main assumptions for the establishment of the model were addressed and their impact was analyzed. Bartrons et al. (2019) modeled the growth and densification of frost based on a fixed grid finite volume approach. Their model accounted for sublimation and solidification. It was concluded that denser meshing should be used for more accurate predictions. A numerical analysis of an ASHP fin and tube evaporator was performed by Popovac et al. (2021) for an algebraic frosting model selected from the literature. The existing model was modified by focusing its execution into 3D general purpose CFD code for unstructured finite volume. The predictions for the frost growth and relative increase in frost mass were compared with experimental results which showed an error of 10%.

Frosting models may predict frost growth, while defrost models extends into predicting the melting process; together they allow optimization of defrosting controls. We therefore present defrosting models next.

## 2.2 Defrost Models

Frost formation and growth on the heat exchanger surface reduces the performance of an ASHP, requiring defrosting to regain normal operation. The defrosting process is complex and affected by many parameters (Steiner & Rieberer, 2013). The stochastic nature of defrosting increases modeling complexity so it is essential to idealize the defrosting process (Qiao et al., 2018). Models provide a means of quantitative analysis for predicting the performance of an air conditioning system (Krakow et al., 1993a). .

Few models for defrosting are available since it involves spatial and time variations (Song et al., 2020). Machielsen & Kerschbaumer (1989) studied the performance of an air cooler under frosting and defrosting conditions. Dimensionless numbers were derived to predict the optimum time for cooling prior to defrost initiation. The defrosting process was divided into three phases: (1) Heat load provided by the refrigerant increases the wall temperature up to 0 ºC, (2) The frost layer starts to melt forming an air gap, and (3) The air gap increases destabilizing the frost layer and melting it away completely. Krakow et al., (1993a) presented an idealized analytical model for reverse cycle defrosting. The model indicated that the pressure-side volumes, the compressor capacity, and the flow characteristic of the throttling device are primary parameters for determining the defrosting characteristics to develop an idealized model for reverse cycle defrosting. Krakow et al. (1993b) experimentally investigated defrosting phenomenon for validating an idealized analytical model. The experimental results were compared with simulation results, and it was concluded that the model is suitable for predicting the system performance during defrost cycles.

Distributed modeling using a capillary for expansion during defrosting was performed by Liu et al. (2003) for an ASHP considering the condenser and evaporator. The modeling results were in good agreement with experimental results excluding the heat stored in the compressor which can affect the defrosting cycle. Hoffenbecker et al. (2005) developed a transient model predicting the effect of heat and mass transfer during hot gas defrost. The model predicted overall time for defrosting of 10 min and 45s which is in good agreement with the field qualitative observation of 10 min for defrosting evaporator. It was concluded that the model is capable to estimate the defrosting energy. A detailed transient model was developed by Dopazo et al. (2010) for six different stages during defrosting. The model predicted the actual time for defrost within less than 2.5% of the experimental data. The model predicted that time for defrosting increases as the mass flow rate of the refrigerant decreases.

A modeling study was performed by Qu et al. (2012) for four stages of defrosting. The model demonstrated a defrost process for multiple circuits. It was concluded that the downward flow of melted frost prolongs the defrosting of the lower circuit, increasing overall defrost duration. Defrosting efficiency e.g. ratio of consumed energy for melting and vaporizing the ice and total supplied energy was found to increase by 18.3% if the melted frost is drained away locally. Steiner & Rieberer (2013) performed transient modeling, evaluating the impact of different parameters during defrosting and optimization of defrosting process. They found that defrost time and defrosting efficiency were affected by throttle valve opening. Song et al. (2020) developed two models for defrosting with both a single drain as well as local drainage for each circuit. They found that local drainage of melted frost reduced the energy consumption by 18.9%.

A modified hot gas defrosting model eliminating the mass non-conservation problem is presented by Han et al. (2022). The operation maps showed that shorter defrost time with low energy consumption can be achieved by maintaining the electronic expansion valve and compressor frequency within 40- 60 % and 70-90 Hz, respectively. Pu et al. (2022) investigated the effect of homogenizing the uneven frost during defrosting operations. If the surface temperature of the outdoor coil is optimized to uniform surface temperature distribution, then the maximal temperature causing frost can be reduce by 2.5 ℃ and minimal relative humidity causing frost can be increase about 5% to 10%.

Defrost modeling for ASHP were identified as a research gap by (Qiao et al., 2018), because there are only few modeling studies in the open literature. RCD is currently the standard defrosting method used for ASHPs, effectively switching the ASHP into AC mode during defrosting. No heating is provided to the indoor space during RCD, which may adversely affect the thermal comport of the occupants.

## 3. FROST RETARDING

The heat pump performance can be improved by delaying frost emerging on the evaporator surface through modifications of system, alteration of the outdoor coil structure, and/or coating of the outdoor coil surface.

### 3.1 System Adjustment

Refrigerant injection, direct injection of refrigerant from condenser outlet to compressor suction line, has been investigated since 1946 due to its capability of retarding frost and improving COP (Winandy & Lebrun, 2002). This method is relatively simple to use and this method consisting of both vapor and liquid injection. However, vapor injection is more efficient than liquid injection (J. Wang et al., 2020). Kang et al. (2018) conducted an experimental experiment to evaluate the effect of vapor injection on the heating capacity and coefficient of performance (COP) of a variable refrigerant flow rate heat pump. A comparison was made between non-vapor injection, single vapor injection, and double vapor injection. Their captured data revealed that both heating capacity and COP improved using double vapor injection compared to single vapor injection. For instance, heating capacity and COP increased by 18.9% and 9.8%, respectively, at compressor frequency of 150 Hz. Bach et al. (2014) found that the capacity increase of the vapor injected ASHP system configuration is the main advantage from a seasonal performance perspective.

### 3.2 Outdoor Coil Structure Modification

Outdoor coil structure plays a crucial role for frost formation duration, and alterations may prolong the frost build-up on the surface. ASHP performance was measured for different fin spacing by Yan et al. (2003), showing good agreement with Zhang et al. (2018). Both found higher fin pitches increased heating capacity and reduced frost formation on the outdoor coils. Fin modification can make the airflow turbulent, as a result, the heat transfer rate increases. Sommers & Jacobi (2005) added vortex generators to fins. This increased the heat transfer rate by 60.6% for the enhanced heat exchanger. Changing fin types and varying geometric parameters can affect frost retardation. An experimental study by Huang et al. (2014) found that flat fins had the best thermal performance, followed by wavy and louvered fins. Furthermore, they found better thermal performance (heat transfer rate) to reduce frosting.

### 3.3 Evaporator Surface Coatings

Surface treatments has recently seen increased attention for frost retardation and removal. Droplet contact angles on hydrophobic, hydrophilic, and bare surfaces of 156.8°, 13.7°, and 95.3° were investigate experimentally by Wang et al. (2018). They found heat transfer rate for hydrophobic surface to be highest followed by hydrophilic and bare surfaces. Total energy consumption for defrosting for bare surface and hydrophilic surface were 163% and 89% more than hydrophobic surface, respectively. Similarly, Abbas & Woo (2021) found that, for the hydrophobic surface, droplets stuck together, and made needle shape crystals, so the frost density was lower than the bare and hydrophilic surface. This led to delay on frost built-up on the outdoor coil surface.

Frost morphology changes of the surface were investigated by Kim & Lee (2011). They found that a hydrophobic surface can not only delay frost formation but can also decrease defrosting time. Frost retardation and defrosting acceleration can also be seen in hydrophilic surface compared to the bare surface; however, it is less effective than hydrophobic surface. Wang et al. (2015) showed good agreement with previous studies on frost retardation of surface modification. Table 1 shows that ice total mass accumulation, thickness, and total heat transfer were affected by surface treatment.

**Table 1:** Attained data from experimental tests of Wang et al. (2015) study

| | **Hydrophobic surface** | **Hydrophilic surface** | **Bare surface** |
|---|---|---|---|
| **Frost thickness (mm) (after 20 min)** | 0.68 | 0.75 | 0.82 |
| **Frost mass (kg) (after 80 min)** | 0.215 | 0.262 | 0.302 |
| **Total heat transfer (kJ)** | 3047.2 | 2667.9 | 2437.7 |

# 4. FROST DETECTION METHODS

ASHP efficiency is degraded by frost on the evaporator surface; frost removal through defrosting is therefore essential. Before initiating a defrost process, frosting needs to be detected. Three major frost detection method groups were identified: (1) Direct methods, (2) Indirect methods, and (3) Prediction based methods (Amer & Wang, 2017).

## 4.1 Direct Methods

Direct methods directly touch the frost or connect with frost to detect it. The capacitive method measures the capacitance difference between electrodes in three conditions: (1) frost-free, (2) water, and (3) frost. The ice, water, and air permittivity differ, so capacitance varies as the frost forms on the evaporator surface (Shen & Wang, 2019).

Transmission type optical sensors comprise two separate sensors; one for emitting infrared rays and one for receiving the rays. When frost accumulates on the surface, received infrared light intensity decreases because it passes the ice which absorbs a portion of the light. Reflective sensors mount both emitter and receiver in the same sensor housing and measures the time delay between emitted light and reflected light to detect the frost ( Wang et al., 2013).

Malik et al. (2020) developed a new model and deployed both optical and capacitive methods simultaneously. Their new model was capable of directly measuring the frost thickness between 1.3 to 8 mm. It was reported that using these two methods at the same time increases the accuracy and reliability of the measurement. Their data from experiments indicated that their measurement method's accuracy varied within a ±5% margin.

Resistive sensors, made of 2 electrodes which the distance between those equal to fins gap, use resistance characteristic of frost to detect frosting. Caetano et al. (2018) conducted an experimental examination to find out the capability of the resistive sensor for frost detection. According to their experiment, resistive sensors could differentiate water and frost because of their different resistance. A piezoelectric sensor was deployed by Roy et al. (1998) to detect frost buildup on the evaporator surface by utilizing the difference in piezoelectric plate frequency in the presence of ice, water, or air. The frequency of the transducer changed from 14 kHz to 28 kHz, while frost thickness increased from 0.06 mm to 0.45 mm.

## 4.2 Indirect Methods

Several techniques can be categorized as indirect methods like pressure drop and image processing methods. These methods never touch or sense the frost for detection purposes. As the frost grows on the evaporator surface, the air flow pathways are obstructed, increasing the pressure drop between inlet and outlet of the heat exchanger pressure drop increased by 600% compared to the initial condition (Rafati et al., 2016). .

Image processing uses one or multiple cameras observing changes to the coil surface to detect frost. Li et al. (2021) conducted a feasibility study for this method for ASHPs. The presence of frost made pictures brighter and was considered a suitable proxy for frost thickness. However, the cameras are a substantial cost factor, and their lenses may require frequent cleaning

## 4.3 Prediction Based Methods

Li et al. (2021) developed a quantitative method to estimate frost thickness and other frost characteristics, using a frost morphology map. After comparing the prediction with experimental data, it was found that their model was 24% more accurate than other prediction-based methods in estimating frost characteristics, thickness, and thermal conductivity.

# 5. DEFROSTING METHODS

Several defrost methods that have been employed by researchers, including hot gas bypass defrosting (HGBD), reverse cycle defrosting (RCD), electric heating defrosting, compressor shut down defrosting, and hot water spraying defrosting (Nawaz et al., 2018). Most of the mentioned methods are nor cost effective neither energy efficient enough to be used in the industry. The most common defrosting method in ASHP applications is RCD followed by HGBD.

## 5.1 Reverse Cycle Defrost Method

The reverse cycle defrost method (RCD), Figure 1, reverses the operating mode from heating to cooling, usually with a 4-way valve. The role of the outdoor coil changes to condenser and the indoor coil works as an evaporator. Heat extracted from the indoor space is moved to the outdoor coil to melt the frost. According to published literature, this procedure can cause a deterioration in the indoor thermal comfort, one of the main problems of this method compared to other methods (Nawaz et al., 2018). The advantages over other defrosting methods include a short defrosting time, high defrosting efficiency (the ratio of ideal energy needed for complete defrosting to actual energy consumed for complete defrosting), and a high COP for a full frosting-defrosting cycle of the system.

Dong et al. (2012) conducted experimental research to evaluate the RCD method. Tests were run for 180 min in pre-defined different conditions to induce ice on the evaporator surface. After reaching 180 min, the four-way valve reversed the flow rate. The indoor fan was maintained to extract sufficient energy from indoor space for defrosting. Their results demonstrated that defrosting efficiency can be increased up to 60% using the RCD method. Also, they found that about 71% of energy for defrosting was provided by indoor air, which caused an indoor thermal comfort decline. Li et al. (2021) investigated the RCD method in electric vehicles' air side heat pumps (ASHP). They pointed out reducing energy consumption over other methods such as HGBD.

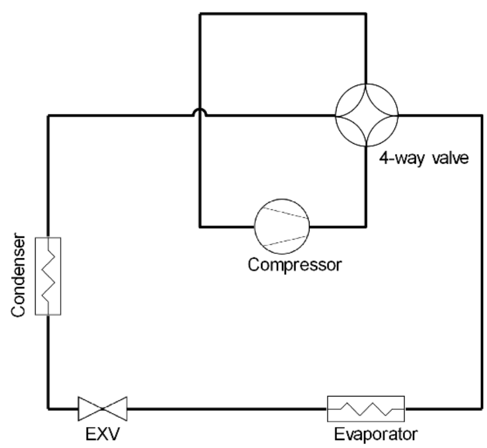


**Figure 1:** System schematic of RCD method

### 5.2 Hot Gas Bypass Defrost Method

The hot gas bypass method for defrosting is commonly used in commercial heat pumps, see figure 2 for the schematic. The pressurized and hot refrigerant, which is in a gas state, directly passes to the evaporator coil to melt the formed frost. Hot refrigerant condenses in the evaporator coil and releases its latent energy to melt the frost. HGBD also has a comparatively short defrosting time in comparison to other methods excluding RCD. Xi et al. (2021) carried out research where the HGBD method was used as defrosting technique. It was found that hot gas bypass defrosting had a 10.17% higher heating capacity and a 4.06% higher overall energy efficiency compared to electric defrosting. The indoor air temperature fluctuates within a range of within 1°C to 1.6°C, which is approximately 84% lower than electric defrosting.

Huang et al. (2009) made a comparison between hot gas bypass and reverse cycle defrost methods as the two most common methods for defrosting. They figured out that, although defrosting time is longer in HGBD than RCD, it is better to use because there is less noise from the refrigerant and less fluctuation in the indoor temperature.

## 6. DEFROST INITIATION STRATEGY

One of the most challenging procedures in heat pumps is defrosting initiation timing, as both an early and a late defrost initiation will reduce energy efficiency; this section presents the relevant defrost initiation strategies.

### 6.1 Time and Time-Temperature Based Methods

The most basic method for controlling defrosting is time-temperature defrost control. This method is based on a predefined schedule for initiating and finishing the defrosting. With a fixed defrosting duration, it is unclear if frost is always fully removed. Adding a surface temperature control alongside a timer to the system can improve the method's reliability, called Temperature-Time control method. The defrost process is started or terminated when the surface temperature attains a predefined temperature or when the preset defrost initiation time is reached. The main problem of this method is that the defrosting process can begin without any frost presence on the evaporator surface. Time-Temperature defrosting control is more commonly used in ASHPs because of its low initial cost, straightforward control, and simple operation (Song et al., 2018).

Pressure sensors also can be utilized instead of temperature sensors to help start or terminate the defrosting process. In the Pressure-Time defrost control strategy, defrosting begins when the difference between evaporator inlet and outlet pressure reaches a predefined value. The defrosting is halted in this method whenever the pressure drop or timer meets the predefined criteria. However, this method has some serious drawbacks versus the Temperature-Time approach, including higher initial cost, lower accuracy, and higher maintenance cost (Nawaz et al., 2018).

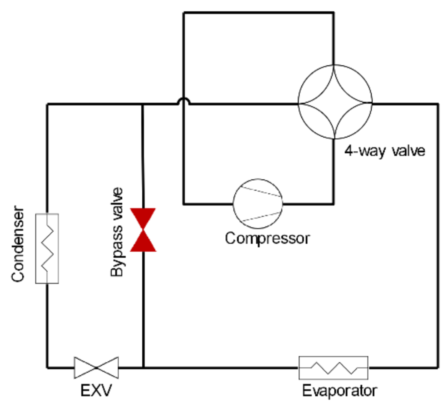


**Figure 2:** System schematic of HGBD method

### 6.2 Artificial Intelligence

With the advent of artificial intelligence (AI), many scholars have started to explore AI to control the frost and defrost process. Sensors acquire ASHP operational data that used by the control system to execute learned logic. Any flaws in training process or training data can lead to robustness issues and malfunctions.

Wang et al. (2021) utilized the convolutional neural network (CNN) method to predict the best time for defrost initiation based on internal operational parameters. First, they imported a set of correct data from a time-based defrosting controlled ASHP. 18 parameters were used to predict the accurate defrost onset time, which only 4 parameters were added to the conventional ASHP data acquisition. Wang et al. (2021)assumed that frost accumulation occurred linearly. The CNN method was used for 6 different cases and the accuracy of this method on defrosting onset varied between 2% to 12%.

## 7. CONCLUSION

Heat pumps (ASHPs) are an important part of contemporary buildings and industry because of their environmentally friendly performance. Whenever ASHPs are operating in heating mode and subject to cold weather, frost can build up on the evaporator surface. This drastically reduces the heat pumps performance, requiring energy costly defrosting. To reduce the energy impact, frost formation can be delayed, e.g. by changing the fin-type, altering the fin gaps, and modifying the surface wettability.

The first step for defrosting is discovering whether how much frost has formed on the heat exchanger surface. Frost detection methods are categorized into direct, indirect, and prediction-based methods. The defrosting procedure should be initiated to remove frost from the outdoor coil after the effect of frost on the outdoor coil exceeds a certain amount, that significantly deteriorates the heat pump COP. Several defrosting methods have been invented, but reverse cycle defrost, and hot gas bypass defrost methods are the most common in both research and industry. They have a reasonable defrost efficiency and short time of the defrosting procedure. Some strategies have been utilized to avoid wasting energy to find the optimum time for defrosting onset. Time-temperature based, artificial intelligence, and optical sensor are the most prevalent methods for defrost detection. Although the time-based methods are not capable of high accuracy in finding the best time for defrosting, they are cheap and robust.

## 8. POTENTIAL FUTURE STUDIES

Although there are several research on the frosting and defrosting of ASHP, many other investigations can be conducted to improve systems performance and reliability. One of the surveys that needs to be done by scholars is finding a robust and near-optimal defrosting initiation and termination algorithm for ASHPs. Additionally, reporting on hybrid methods (mixing of two existing or new method) for frost retardation, frost detection, and defrosting initiation are missing in papers. Hybrid methods are beneficial because the accuracy and credibility of the experiment tremendously increase.

## REFERENCES

Abbas, S., & Woo, C. (2021). Frosting and defrosting assessment of carbon fiber reinforced polymer composite with surface wettability and resistive heating characteristics. *IJHMT*, *169*, 120883.

Amer, M., & Wang, C. (2017). Review of defrosting methods. *Renewable and Sustainable Energy Reviews*, 73 (October 2016), 53–74.

Bach, C. K., Groll, E. A., Braun, J. E., Horton, W. T., Jischke, S. M., & Lafayette, W. (2014). *Effects of Vapor Injected Compression , Hybrid Evaporator Flow Control , and Other Parameters on Seasonal En. Eff.* International Refrigeration and Air Conditioning Conference, 1–11.

Bartrons, E., Galione, P. A., & Pérez-Segarra, C. D. (2019). Fixed grid numerical modelling of frost growth and densification. *IJHMT*, 130, 215–229.

Brèque, F., & Nemer, M. (2016). Modélisation du givrage sur une plaque plane froide: Comparaison des différentes hypothèses et impacts sur les prévisions de croissance de givre. *IJIR*, 69, 340–360.

Caetano, D., Gaspar, P. D., & Dinho, P. (2018). Smart ice detection systems based on resonant piezoelectric transducers. *VII Congreso Iberoamericano de Las Ciencias y Técnicas Del Frío*, 19–21.

Dong, J., Deng, S., Jiang, Y., Xia, L., & Yao, Y. (2012). An experimental study on defrosting heat supplies and energy consumptions during a reverse cycle defrost operation for an air source heat pump. *ATE*, *37*, 380–387.

Dopazo, J. A., Fernandez-Seara, J., Uhía, F. J., & Diz, R. (2010). Modelling and experimental validation of the hot-gas defrost process of an air-cooled evaporator. *JIJR*, 33(4), 829–839.

Han, B., Xiong, T., Xu, S., Liu, G., & Yan, G. (2022). Parametric study of a room air conditioner during defrosting cycle based on a modified defrosting model. *Energy*, 238, 121658.

Hoffenbecker, N., Klein, S. A., & Reindl, D. T. (2005). Hot gas defrost model development and validation. *JIJR*, 28(4), 605–615.

Huang, D., Li, Q., & Yuan, X. (2009). Comparison between hot-gas bypass defrosting and reverse-cycle defrosting methods on an air-to-water heat pump. *Applied Energy*, *86*(9), 1697–1703.

Huang, D., Ri-Jing, Z., Liu, Y., & Yi, D.-B. (2014). Effect of fin types of outdoor fan-supplied finned-tube heat exchanger on periodic frosting and defrosting performance of a residential air-source heat pump. *ATE*, 69(1), 251–260.

Jianhui, N., Guoyuan, M., & Shuxue, X. (2020). Experimental study on the performance of air source heat pump system with multiple parallel outdoor units. *IJER*, 44(4), 2819–2832.

Kang, D., Jeong, J. H., & Ryu, B. (2018). Heating performance of a VRF heat pump system incorporating double vapor injection in scroll compressor. *JIJR*, 96, 50–62.

Kim, J. S., Yang, D. K., & Lee, K. S. (2008). Dimensionless correlations of frost properties on a cold cylinder surface. *IJHMT*, 51(15–16), 3946–3952.

Kim, K., & Lee, K.-S. (2011). Frosting and defrosting characteristics of a fin according to surface contact angle. *IJHMT*, 54(13), 2758–2764.

Kim, M., & Lee, K. (2015). Determination method of defrosting start-time based on temperature measurements. *Applied Energy*, 146, 263–269.

Krakow, K. I., Lin, S., & Yan, L. (1993a). Idealized model of reversed-cycle hot gas defrosting. Part 1: Theory. *ASHRAE Transactions*, 99(pt 2), 317–328.

Krakow, K. I., Lin, S., & Yan, L. (1993b). Idealized model of reversed-cycle hot gas defrosting. Part 2: Experimental analysis and validation. *ASHRAE Transactions*, 99(pt 2), 329–338.

Lee, K. S., Kim, W. S., & Lee, T. H. (1997). A one-dimensional model for frost formation on a cold flat surface. *IJHMT*, 40(18), 4359–4365.

Li, K., Xia, D., Bao, J., Luo, S., Zhang, H., Liu, N., Su, L., & Sheng, L. (2021). Investigation on reverse cycle defrosting strategy of an outdoor heat exchanger in air conditioning heat pump system for electric vehicles. *Case Studies in Thermal Engineering*, 27, 101281.

Li, Z., Wang, W., Sun, Y., Wang, S., Deng, S., & Lin, Y. (2021). Applying image recognition to frost built-up detection in air source heat pumps. *Energy*, 233, 121004.

Liu, Z., Tang, G., & Zhao, F. (2003). Dynamic simulation of air-source heat pump during hot-gas defrost. *ATE*, 23(6), 675–685.

Machielsen, C. H. M., & Kerschbaumer, H. G. (1989). Influence of frost formation and defrosting on the performance of air coolers: standards and dimensionless coefficients for the system designer. *JIJR*, 12(5), 283–290.

Malik, A. N., Khan, S. A., & Lazoglu, I. (2020). A novel hybrid frost detection and defrosting system for domestic refrigerators. *JIJR*, 117, 256–268.

Mengjie, S., Shiming, D., Chaobin, D., Ning, M., & Zhihua, W. (2018). Review on improvement for air source heat pump units during frosting and defrosting. *Applied Energy*, *211*(December 2017), 1150–1170.

Nawaz, K., Elatar, A., & Fricke, B. (2018). *A Critical Literature Review of Defrost Technologies for Heat Pumps and refrigeration system*. Oak Ridge National Laboratory.

Negrelli, S., & Hermes, C. J. L. (2015). A semi-empirical correlation for the thermal conductivity of frost. *JIJR*, 58, 243–252.

Popovac, M., Emhofer, J., & Reichl, C. (2021). Frosting in a heat pump evaporator part B: Numerical analysis. *ATE*, 199(August), 117488.

Pu, J., Shen, C., Zhang, C., & Yan, X. (2022). A semi-experimental investigation on the anti-frosting potential of homogenizing the uneven frosting for air source heat pumps. *Energy and Buildings*, *260*, 111939.

Qiao, H., Aute, V., & Radermacher, R. (2018). Modeling of transient characteristics of an air source heat pump with vapor injection during reverse-cycle defrosting. *JIJR*, 88, 24–34.

Qu, M., Pan, D., Xia, L., Deng, S., & Jiang, Y. (2012). A study of the reverse cycle defrosting performance on a multi-circuit outdoor coil unit in an air source heat pump - Part II: Modeling analysis. *A. Energy*, *91*(1), 274–280.

Rafati, M., Fathieh, F., Kadylak, D., Huizing, R., Besant, R. W., & Simonson, C. J. (2016). Experimental methods for detecting frosting in cross-flow air-to-air energy exchangers. *Exp. Thermal and Fluid Sc.*, 77, 100–115.

Reiners, T., Gross, M., Altieri, L., Wagner, H.-J., & Bertsch, V. (2021). Heat pump efficiency in fifth generation ultra-low temperature district heating networks using a wastewater heat source. *Energy*, 236, 121318.

Roy, S., Izad, A., Deanna, R. G., & Mehregany, M. (1998). Smart ice detection systems based on resonant piezoelectric transducers. *Sensors and Actuators A: Physical*, 69, 243–250.

Şahin, A. Z. (1995). An analytical study of frost nucleation and growth during the crystal growth period. *Heat and Mass Transfer*, 30(5), 321–330.

Shen, Y., & Wang, X. (2019). Real-time frost porosity detection using capacitance sensing approach. *IJHMT*, 134, 1171–1179.

Sommers, A. D., & Jacobi, A. M. (2005). Air-side heat transfer enhancement of a refrigerator evaporator using vortex generation. *JIJR*, 28(7), 1006–1017.

Song, M., Fan, C., Mao, N., & Xu, Y. (2018). Energy & Buildings An experimental study on time-based start defrosting control strategy optimization for an air source heat pump unit with frost evenly distributed and melted frost locally drained. *Energy & Buildings*, 178, 26–37.

Song, M., Xie, G., Pekař, L., Mao, N., & Qu, M. (2020). A modeling study on the revere cycle defrosting of an air source heat pump with the melted frost downwards flowing away and local drainage. *Energy and Buildings*, 226, 110257.

Steiner, A., & Rieberer, R. (2013). Parametric analysis of the defrosting process of a reversible heat pump system for electric vehicles. *ATE*, 61(2), 393–400.

Tang, J., Hu, X., Herman, C., & Gong, G. (2020). Computational modeling and prediction of the performance of air source heat pumps under frost prevention and retardation conditions. *Energy and Buildings*, *224*, 110264.

Wang, F., Liang, C., Yang, M., Fan, C., & Zhang, X. (2015). Effects of surface characteristic on frosting and defrosting behaviors of fin-tube heat exchangers. *ATE*, 75, 1126–1132.

Wang, F., Liang, C., Zhang, X., & Zhang, Y. (2018). E ff ects of surface wettability and defrosting conditions on defrosting performance of fi n-tube heat exchanger. *Exp. Thermal and Fluid Sc.*, 93(September 2017), 334–343.

Wang, J., Qv, D., Ni, L., & Yao, Y. (2020). Experimental study on an injection-assisted air source heat pump with a novel two-stage variable-speed scroll compressor. *ATE*, 176, 115415.

Wang, W, Feng, Y. C., Zhu, J. H., Li, L. T., Guo, Q. C., & Lu, W. P. (2013). Performances of air source heat pump system for a kind of mal-defrost phenomenon appearing in moderate climate conditions. *Applied Energy*, 112, 1138–1145.

Wang, W, Xiao, J., Guo, Q. C., Lu, W. P., & Feng, Y. C. (2011). Field test investigation of the characteristics for the air source heat pump under two typical mal-defrost phenomena. *Applied Energy*, 88(12), 4470–4480.

Wang, Wei, Xiao, J., Feng, Y., Guo, Q., & Wang, L. (2013). Characteristics of an air source heat pump with novel photoelectric sensors during periodic frost–defrost cycles. *ATE*, 50(1), 177–186.

Wang, Wenyi, Zhou, Q., Tian, G., Wang, Y., Zhao, Z., & Cao, F. (2021). A novel defrosting initiation strategy based on convolutional neural network for air-source heat pump. *JIJR*, 128, 95–103.

Winandy, E. L., & Lebrun, J. (2002). Scroll compressors using gas and liquid injection: experimental analysis and modelling. *JIJR*, 25(8), 1143–1156.

Tao, X., R. W. B. and K. S. R. (1992). *A mathematical model for predicting the densification and growth of frost on a flat plate Y Department of Mechanical Engineering, University of Saskatchewan. Saskatoon. Saskatchewan S7N OWO, Canada*.

Xi, Z., Yao, R., Li, J., Du, C., Yu, Z., & Li, B. (2021). Experimental studies on hot gas bypass defrosting control strategies for air source heat pumps. *Journal of Building Engineering*, 43(August), 103165.

Yan, W.-M., Li, H.-Y., Wu, Y.-J., Lin, J.-Y., & Chang, W.-R. (2003). Performance of finned tube heat exchangers operating under frosting conditions. *IJHMT*, 46(5), 871–877.

Yang, D. K., Lee, K. S., & Cha, D. J. (2006). Frost formation on a cold surface under turbulent flow. *JIJR*, 29(2), 164–169.

Yun, R., Kim, Y., & Min, M. K. (2002). Modeling of frost growth and frost properties with airflow over a flat plate. *JIJR*, *25*(3), 362–371.

Zhang, L., Jiang, Y., Dong, J., Yao, Y., & Deng, S. (2018). An experimental study of frost distribution and growth on finned tube heat exchangers used in air source heat pump units. *ATE*, *132*, 38–51.

## ACKNOWLEDGMENT

This research is funded by OCAST OARS Award AR21-071-1 and AAON, Inc.